Radiation tests of real-sized prototype RPCs for the Phase-2 Upgrade of the CMS Muon System

2016 JINST 11 C08008

(http://iopscience.iop.org/1748-0221/11/08/C08008)

Published by IOP Publishing for Sissa Medialab

Received: *May 6, 2016*
Revised: *July 6, 2016*
Accepted: *July 28, 2016*
Published: *August 10, 2016*

13th Workshop on Resistive Plate Chambers and Related Detectors,
22–26 February 2016,
Ghent, Belgium

2016 JINST 11 C08008

Radiation tests of real-sized prototype RPCs for the Phase-2 Upgrade of the CMS Muon System

K.S. Lee,[a,1] S.W. Cho,[a] S.Y. Choi,[a] B. Hong,[a] Y. Go,[a] M.H. Kang,[a] J.H. Lim,[a] S.K. Park,[a] A. Cimmino,[b] S. Crucy,[b] A. Fagot,[b] M. Gul,[b] A.A.O. Rios,[b] M. Tytgat,[b] N. Zaganidis,[b] S. Aly,[c] Y. Assran,[c] A. Radi,[c] A. Sayed,[c] G. Singh,[d] M. Abbrescia,[e] G. Iaselli,[e] M. Maggi,[e] G. Pugliese,[e] P. Verwilligen,[e] W. van Doninck,[f] S. Colafranceschi,[g] A. Sharma,[g] L. Benussi,[h] S. Bianco,[h] D. Piccolo,[h] F. Primavera,[h] V. Bhatnagar,[i] R. Kumarl,[i] A. Metha,[i] J. Singh,[i] A. Ahmad,[j] M. Ahmad,[j] W. Ahmed,[j] M.I Asghar,[j] I.M. Awan,[j] Q. Hassan,[j] H. Hoorani,[j] W.A. Khan,[j] T. Khurshid,[j] S. Muhammad,[j] M.A. Shah,[j] H. Shahzad,[j] M.S. Kim,[k] M. Goutzvitz,[l] G. Grenier,[l] F. Lagarde,[l] I.B. Laktineh,[l] S. Carpinteyro Bernardino,[m] C. Uribe Estrada,[m] I. Pedraza,[m] C.B. Severiano,[m] S. Carrillo Moreno,[n] F. Vazquez Valencia,[n] L.M. Pant,[o] S. Buontempo,[p] N. Cavallo,[p] M. Esposito,[p] F. Fabozzi,[p] G. Lanza,[p] L. Lista,[p] S. Meola,[p] M. Merola,[p] I. Orso,[p] P. Paolucci,[p] F. Thyssen,[p] A. Braghieri,[q] A. Magnani,[q] P. Montagna,[q] C. Riccardi,[q] P. Salvini,[q] I. Vai,[q] P. Vitulo,[q] Y. Ban,[r] S.J. Qian,[r] M. Choi,[s] Y. Choi,[t] J. Goh,[t] D. Kim,[t] A. Aleksandrov,[u] R. Hadjiiska,[u] P. Iaydjiev,[u] M. Rodozov,[u] S. Stoykova,[u] G. Sultanov,[u] M. Vutova,[u] A. Dimitrov,[v] L. Litov,[v] B. Pavlov,[v] P. Petkov,[v] D. Lomidze,[w] C. Avila,[x] A. Cabrera,[x] J.C. Sanabria,[x] I. Crotty[y] and J. Vaitkus[z]

[a] *Korea University, Department of Physics, 145 Anam-ro, Seongbuk-gu, Seoul 02841, Republic of Korea*
[b] *Ghent university, Dept. of Physics and Astronomy, Proeftuinstraat 86, B-9000 Ghent, Belgium*
[c] *Egyptian Network for High Energy Physics, Academy of Scientific Research and Technology, 101 Kasr El-Einy St. Cairo Egypt*
[d] *Chulalongkorn University, Department of Physics, Faculty of Science, Payathai Road, Phatumwan, Bangkok, Thailand - 10330*
[e] *INFN, Sezione di Bari, Via Orabona 4, IT-70126 Bari, Italy*
[f] *Vrije Universiteit Brussel, Boulevard de la Plaine 2, 1050 Ixelles, Belgium*
[g] *Physics Department CERN, CH-1211 Geneva 23, Switzerland*
[h] *INFN, Laboratori Nazionali di Frascati (LNF), Via Enrico Fermi 40, IT-00044 Frascati, Italy*
[i] *Department of Physics, Panjab University, Chandigarh Mandir 160 014, India*

[1] Corresponding author.

doi:10.1088/1748-0221/11/08/C08008

[j] National Centre for Physics, Quaid-i-Azam University, Islamabad, Pakistan
[k] Kyungpook National University, 80 Daehak-ro, Buk-gu, Daegu 41566, Republic of Korea
[l] Universite de Lyon, Universite Claude Bernard Lyon 1, CNRS-IN2P3,
Institut de Physique Nucleaire de Lyon, Villeurbanne, France
[m] Benemerita Universidad Autonoma de Puebla, Puebla, Mexico
[n] Universidad Iberoamericana, Mexico City, Mexico
[o] Nuclear Physics Division Bhabha Atomic Research Centre, Mumbai 400 085, India
[p] INFN, Sezione di Napoli, Complesso Univ. Monte S. Angelo, Via Cintia, IT-80126 Napoli, Italy
[q] INFN, Sezione di Pavia, Via Bassi 6, IT-Pavia, Italy
[r] School of Physics, Peking University, Beijing 100871, China
[s] University of Seoul, 163 Seoulsiripdae-ro, Dongdaemun-gu, Seoul 02504, Republic of Korea
[t] Sungkyunkwan University, 2066 Seobu-ro, Jangan-gu, Suwon-si 16419, Gyeonggi-do, Republic of Korea
[u] Bulgarian Academy of Sciences, Inst. for Nucl. Res. and Nucl. Energy,
Tzarigradsko shaussee Boulevard 72, BG-1784 Sofia, Bulgaria
[v] Faculty of Physics, University of Sofia, 5, James Bourchier Boulevard, BG-1164 Sofia, Bulgaria
[w] Tbilisi University, 1 Ilia Chavchavadze Ave, Tbilisi 0179, Georgia
[x] Universidad de Los Andes, Apartado Aereo 4976, Carrera 1E, no. 18A 10, CO-Bogota, Colombia
[y] Dept. of Physics, Wisconsin University, Madison, WI 53706, United States
[z] Vilnius University, Vilnius, Lithuania

E-mail: kslee0421@korea.ac.kr

Abstract: We report on a systematic study of double-gap and four-gap phenolic resistive plate chambers (RPCs) for the Phase-2 upgrade of the CMS muon system at high η. In the present study, we constructed real-sized double-gap and four-gap RPCs with gap thicknesses of 1.6 and 0.8 mm, respectively, with 2-mm-thick phenolic high-pressure-laminated (HPL) plates. We examined the prototype RPCs with cosmic rays and with 100-GeV muons provided by the SPS H4 beam line at CERN. To examine the rate capability of the prototype RPCs both at Korea University and at the CERN GIF++ facility, the chambers were irradiated with ^{137}Cs sources providing maximum gamma rates of about 1.5 kHz cm^{-2}. For the 1.6-mm-thick double-gap RPCs, we found the relatively high threshold on the produced detector charge was conducive to effectively suppressing the rapid increase of strip cluster sizes of muon hits with high voltage, especially when measuring the narrow-pitch strips. The gamma-induced currents drawn in the four-gap RPC were about one-fourth of those drawn in the double-gap RPC. The rate capabilities of both RPC types, proven through the present testing using gamma-ray sources, far exceeded the maximum rate expected in the new high-η endcap RPCs planned for future phase-II runs of the Large Hadron Collider (LHC).

Keywords: Resistive-plate chambers; Gaseous detectors; Trigger detectors

2016 JINST 11 C08008

Contents

1 Introduction

RPCs are a part of the Compact Muon Solenoid (CMS) [1–4], which plays as an important role in e.g. searches for new physics and in the recent discovery of the Higgs boson [5]. Inside the muon system, RPCs are mainly used as trigger devices, but also contribute to the reconstruction of muons. As illustrated in figure 1, the current CMS RPC system covering a pseudorapidity range of $|\eta| < 1.6$ comprises six trigger stations in the barrel and four trigger stations in the endcap sections of the CMS detector [6, 7]. The fourth RPC trigger station in the endcap section (the zone in the upper-right solid line of figure 1) has been recently installed to reinforce the muon-trigger efficiency of the CMS for the LHC runs, starting in 2015 [8, 9].

The current CMS endcap RPCs comprise 2-mm-thick double-gap chambers, each covering an azimuthal (ϕ) angular range of 10°. Each RPC chamber contains three sectors of 32 trapezoidal strips, each covering a detection range of 0.31° in ϕ and 0.1 in η [4].

The CMS RPC group recently addressed the need for an extension of the RPC system towards higher rapidity (the region in the bottom red box in figure 1) to maintain the present muon trigger performance during the future 14-TeV LHC runs with a maximum luminosity of about 5×10^{34} cm^{-2} s^{-1} [10]. It is expected that these new RPCs (labeled as RE3/1 and RE4/1 in figure 1) will face a beam-related background with a maximum rate of about 600 Hz cm^{-2} in the maximum η division, an order of magnitude increase (by a factor at least 10 times higher) over the background rate previously experienced with the 8-TeV beam with a maximum luminosity of 6×10^{33} cm^{-2} s^{-1} during past LHC operations [11, 12].

Improving the detector sensitivity represents the most relevant solution for proper RPC operations in an environment of a high-rate background. Furthermore, a lower-gain avalanche-mode operation should improve the longevity of the RPC detectors. In the present study, we examined two different types of phenolic RPCs: double-gap and four-gap RPCs, with single-gap thicknesses of 1.6 mm and 0.8 mm, respectively. Four real-sized prototype RPCs (two of each type) with 2-mm-thick phenolic HPL were constructed and tested with muons and gamma sources to probe the detector performances.

Previous reports have described the structure of the four-gap RPCs (each composed of two bi-gaps) [13, 14]. We measured the mean value of the bulk resistivity of the phenolic HPL panels used for the construction of the present prototype RPCs as about 3×10^{10} Ωcm at a temperature of 20°C. Figure 2 shows the layout of 128 readout strips in the prototype RPCs. We adopted the old RE1/1-type geometry for the prototype RPCs because its strip pitches and lengths approximately matched those envisioned for the future RE3/1 and RE4/1 RPCs.

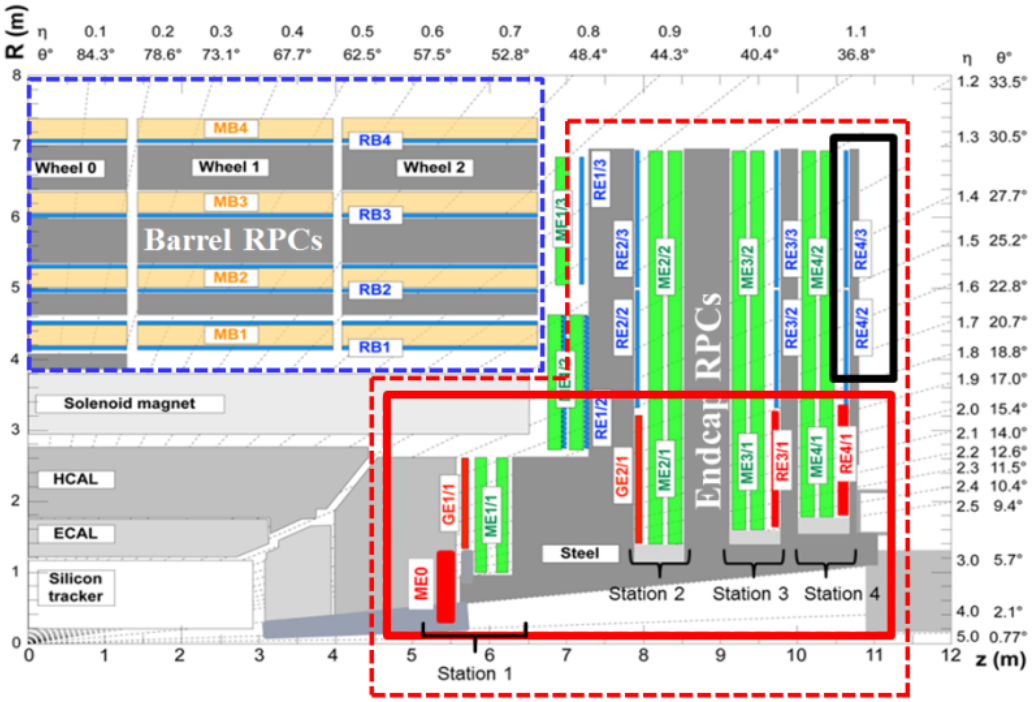

Figure 1. Quadrant of the CMS detector, showing the muon system inside the dashed boxes, with the current RPCs in blue.

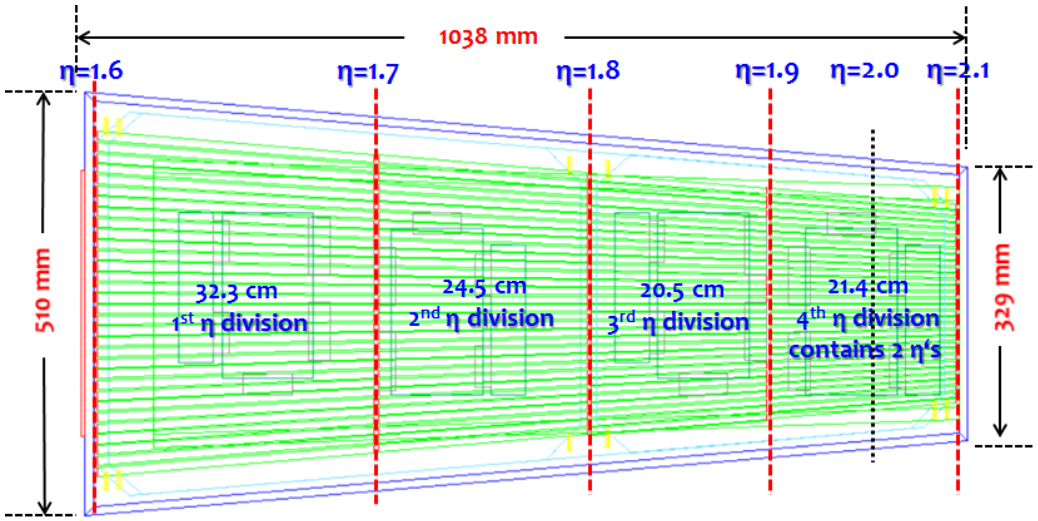

Figure 2. Layout of 128 readout strips in the prototype RPCs constructed with the old RE1/1 type geometry.

2 Test facilities

We tested the prototype RPCs with cosmic rays at Korea University, and in parallel with 100 GeV muons provided by the CERN SPS H4 test beam line. To study the rate capability of the prototype RPCs, they were exposed to ^{137}Cs gamma-ray sources, both at Korea University and at the CERN new Gamma Irradiation Facility (GIF++). The current activity levels of the sources in Korea and in the GIF++ were 5.55 GBq and 13.9 TBq, respectively.

For the radiation test at Korea University, we placed each RPC type at a distance of 36 cm from the source, as shown on the left in figure 3. For the muon-beam test, we placed the two RPC types close together, installed at about 5 m from the GIF++ cesium source, as shown on the right in figure 3.

Figure 3. Prototype RPCs installed at a distance of 36 cm from the 5.55-GBq ^{137}Cs source at Korea University (left), and at about 5 m from the 13.9-TBq ^{137}Cs source at the GIF++ (right).

The signals that arose in the RPC strips were transferred to front-end-electronics (FEE) via 50-Ω coaxial cables. The impedance of the strips illustrated in figure 2 was estimated to be approximately from 20 to 40 Ω. In order to confirm the range of the impedance of the strips whose pitches vary from 7.5 to 13.3 mm, impedance of 30-cm-long, 10-mm-pitch strips embedded in a small 1.6-mm-thick double-gap-type mockup RPC was measured by using a variable resistor and 2-ns-wide triangular pulses provided by a function generator. The value of the impedance was obtained by carefully adjusting the resistance of the variable resistor that yields minimal reflection at the junction of the strip and the resistor connected in series. The mean value of the impedance and the standard deviation for the 10-mm-pitch strips obtained from twenty measurements were measured as 28 and 5 Ω, respectively.

We appropriately delayed the low-voltage differential signaling (LVDS) outputs of the FEEs, transferred to a multi-hit time-to-digital converter (TDC) via 34-pin twisted-pair cables. For the cosmic-muon test at Korea University, we used two different FEE types for the digitization of the signals: charge-sensitive FEEs for the operation of the current CMS RPCs; and voltage-sensitive FEEs developed specifically for the present study of RPCs. For the beam test at the GIF++, we used only CMS RPC FEEs for the digitization. The threshold values for the digitization in the CMS RPC FEEs ranged from 170 to 220 fC. Those applied in the voltage-sensitive FEEs ranged from 0.6 to

2016 JINST 11 C08008

1.0 mV. The gains of amplification in the charge-sensitive (nonlinear) and voltage -sensitive (linear) FEEs are 1.8 mV/fC and 200 mV/mV, respectively.

The gas mixture for the RPC operation used at the GIF++ was composed of 95.2% $C_2H_2F_4$, 4.5% i-C_4H_{10}, and 0.3% SF_6 humidified with a relative humidity of about 40%. For the test at Korea University, we added water vapor with a mass ratio of 0.3% to the same gas mixture.

3 Results

3.1 Threshold dependence

Figure 4 shows detection efficiencies (ε_μ) and mean cluster sizes ($\langle C_s \rangle$) as a function of high voltage for cosmic muons impinging on the first (left) and the third (right) η division of the double-gap RPCs at Korea University. The mean values of the strip pitches for the first and the third η divisions are 12.5 and 8.5 mm, respectively. We labeled the data obtained at the thesholds of 0.6 and 1.0 mV (voltage-sensitive FEEs) and of 180 fC (charge-sensitive FEEs) by open and full circles and inverted triangles, respectively. We converted the applied high voltages to the effective values, HV_{eff}, under the standard conditions of $P = 1013$ hPa and $T = 293$ K [14]. As shown on the right in figure 4, $\langle C_s \rangle$ of the muons measured at the narrower-pitch strips and at the lower threshold appeared especially high and increased more rapidly with HV_{eff}, while ε_μ appeared rather insensitive to the choice of the threshold.

We attributed the rapid increase of $\langle C_s \rangle$ with HV_{eff} in the data in figure 4 to participation of the hits arose by capacitive inductions between the adjacent strips. The relatively higher value of threshold appeared more effective to suppress the magnitude of $\langle C_s \rangle$ especially when the strip pitch was narrower. Nevertheless, fine adjustments of the threshold values in accordance with the strip pitches would be conducive to achieving a consistent hit structure over the whole detector surface.

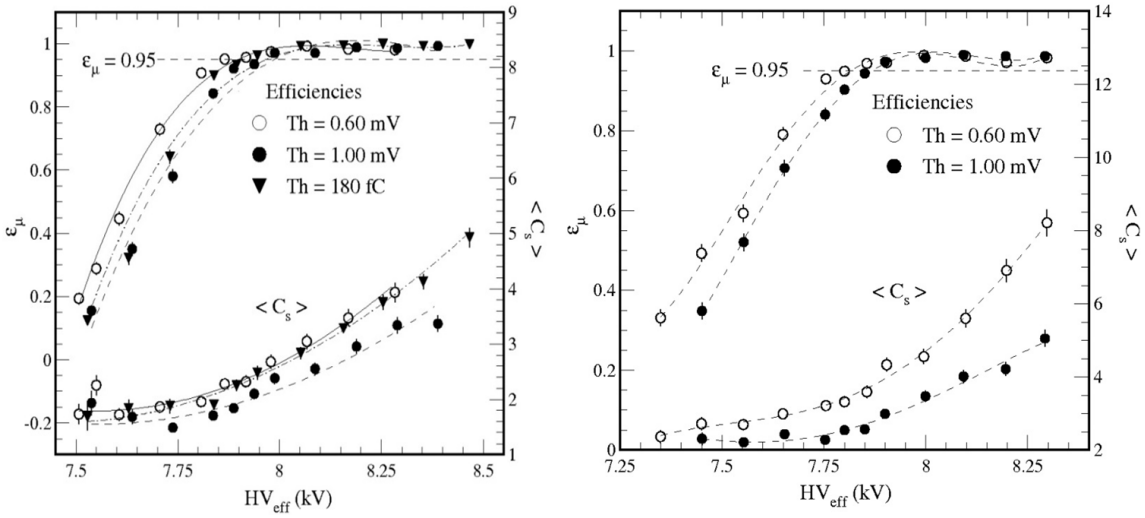

Figure 4. ε_μ and $\langle C_s \rangle$ for cosmic muons as a function of HV_{eff} at Th = 0.6 (open circles) and 1.0 mV (full circles), and Th = 180 fC (inverted triangles), tested for the first (left) and the third (right) η divisions of the double-gap RPCs at Korea University.

2016 JINST 11 C08008

Figure 5 shows ε_μ and $\langle C_s \rangle$ as a function of high voltage, measured with cosmic muons on the first (left) and the third (right) η divisions of the four-gap RPCs, also at Korea University. We labeled the data obtained at the thesholds of 0.6, 0.75, and 1.0 mV by open circles, full circles, and squares, respectively.

In contrast to the case of the double-gap RPCs, both ε_μ and $\langle C_s \rangle$ shift significantly with increasing the threshold value. The relatively larger sensitivity of ε_μ to the threshold for the four-gap RPCs implies an advantage, enhancing the detector sensitivity by lowering the threshold without unnecessarily magnifying the cluster sizes. Lowering the threshold (i.e., enhancing the detector sensitivity) would be conducive to achieving higher rate capability, as well as to improving the longevity of the gas gaps.

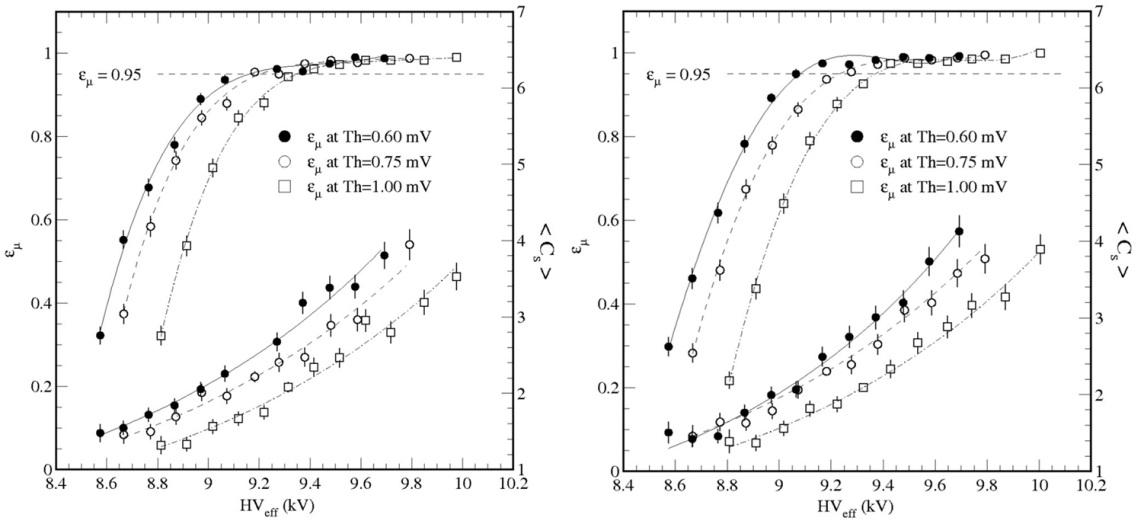

Figure 5. ε_μ and $\langle C_s \rangle$ for cosmic muons as a function of $\mathrm{HV_{eff}}$ at Th = 0.6 (open circles), 0.75 (full circles), and 1.0 mV (squares), tested for the first (left) and the third (right) η divisions of the four-gap RPCs at Korea University.

3.2 Pickup charges

We linearly amplified the pickup signals from the cosmic muons in the two prototype RPCs by a factor 10, before sending them to two 400-MHz four-channel fresh analog-to-digital converters (FADCs). We carefully calibrated the amplitudes of the FADC values using well-defined square pulses provided by a pulse generator. We set the time window allowed for the integration of the charges to 75 ns. The standard deviation (σ) of the pedestal measured at the individual FADC channel ranged from 15 to 25 fC.

Figure 6 shows the pickup-charge distributions of the muon-hit clusters measured on the double-gap RPC at $\mathrm{HV_{eff}}$ = 7.92 kV, 8.09 kV, 8.28 kV, and 8.55 kV (left panels) and on the four-gap RPC at $\mathrm{HV_{eff}}$ = 9.15 kV, 9.38 kV, 9.67 kV, and 9.33 kV (right panels) using the FADCs. The charge spectra in the first panels in the left (double-gap RPC) and in the right (four-gap RPC) yield $\varepsilon_\mu \sim 0.95$ when the muons were measured at Th = 0.6 mV using the TDC.

2016 JINST 11 C08008

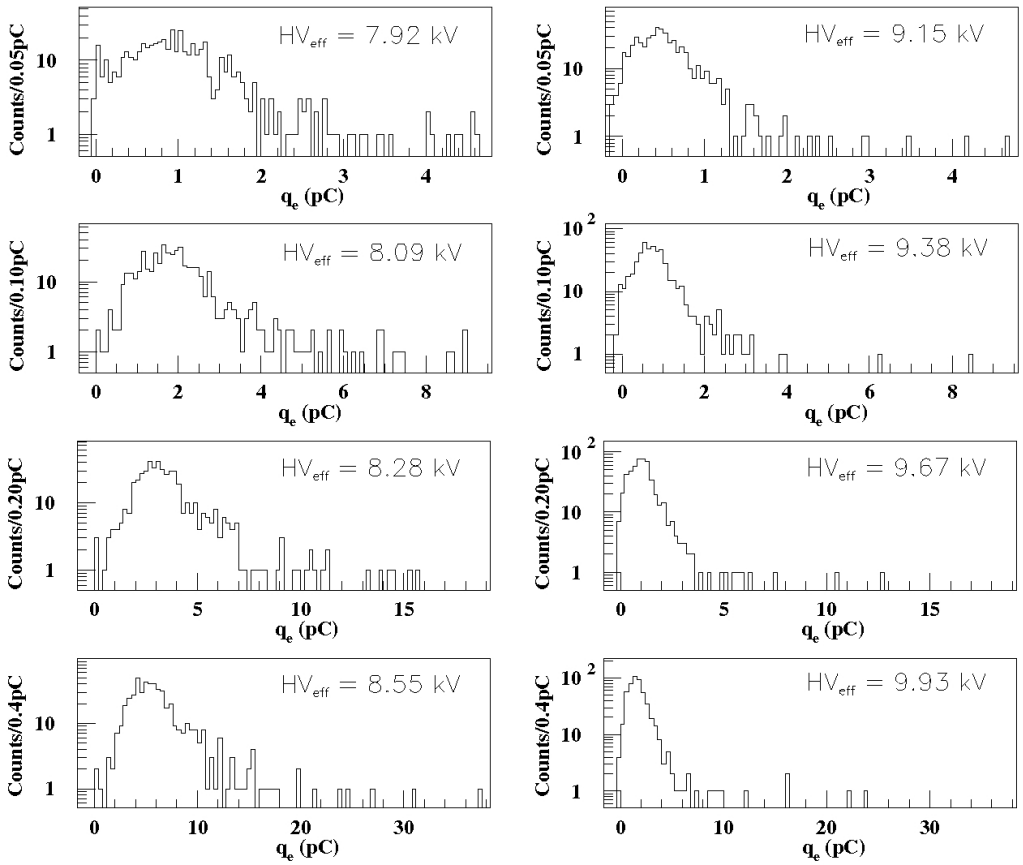

Figure 6. Pickup-charge distributions of the muon-hit clusters measured on the double-gap RPC (left panels) and on the four-gap RPC (right panels) at four different effective high voltages, respectively, using the FADCs.

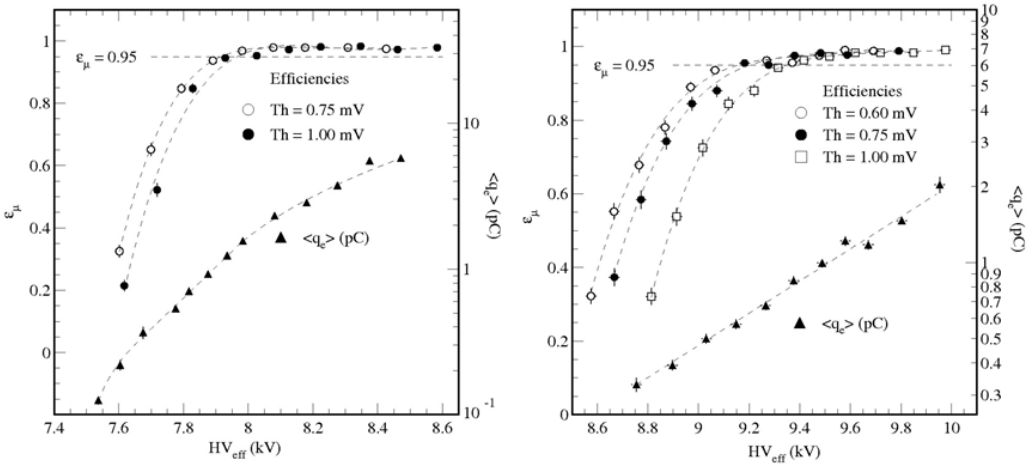

Figure 7. $\langle q_e \rangle$ (triangles) and ε_μ at Th = 0.6 (open circles), 0.75 (full circles), 1.0 mV (squares), tested for the first η divisions of the double-gap (left) and the four-gap (right) RPCs, as a function of HV_{eff}.

Figure 7 shows the mean pickup charges $\langle q_e \rangle$ (triangles, by FADCs) and ε_μ (by TDCs) of the muon-hit clusters as a function of HV_{eff} at Th = 0.6 (open circles), 0.75 (full circles), and 1.0 mV (squares), tested for the first η divisions of the double-gap (left) and the four-gap (right) RPCs. For the double-gap RPCs, the slope of the growth of $\langle q_e \rangle$ decreased continuously with HV_{eff} due to the increasing screening effect of the space charges in the avalanche. When ε_μ reached 0.95, the reduction of the slope became significant, allowing us to obtain the ample plateau size for the operation.

However, the growth of $\langle q_e \rangle$ measured with the four-gap RPCs appeared saturated even at the low HV_{eff}. As the result, we expected that we could effectively shift the dynamic range of operation toward the lower HV_{eff} by lowering the threshold, without losing the significant size of the operational plateau. The current interpretation of the data for the four-gap RPC was also brought up for the development of high sensitive preamplifiers for ATLAS RPCs [15].

3.3 Influence of gamma background

We estimated the gamma-ray flux impinging on the RPCs placed at 36 cm from the 5.55 GBq ^{137}Cs gamma source at Korea University to be 0.32 MHz cm^{-2}. Figure 8 shows ε_μ for the cosmic muons (top symbols scaled on the left axis) and the gamma rates R_γ (bottom symbols scaled on the right axis) at Th = 0.6 (full circles), 0.75 (open circles), and 1.0 mV (squares), as a function of HV_{eff}, tested for the first η divisions of the double-gap (left) and the four-gap (right) RPCs. We labeled the gamma-induced currents drawn in the RPCs as triangles. In the mid-section of efficiency plateau, the gamma-induced currents drawn in the four-gap RPCs were about one fourth of those drawn in the double-gap RPCs. Considering the high particle rates expected in the RE3/1 and RE4/1 RPCs, the smaller avalanche charges of the four-gap RPCs should provide a fair advantage to guarantee longevity.

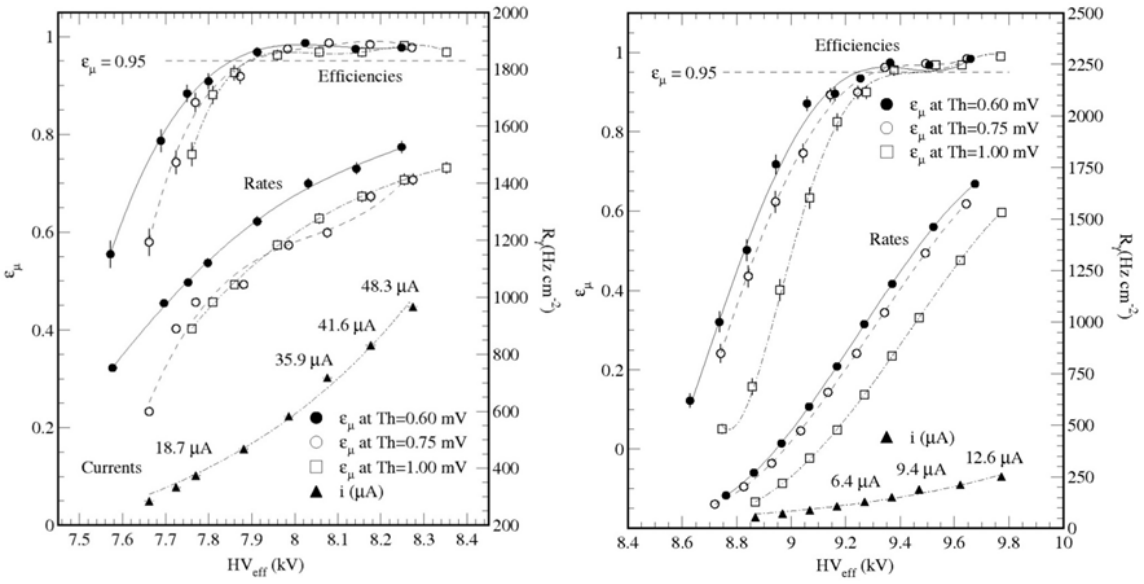

Figure 8. ε_μ for the cosmic muons (top symbols scaled on the left axis) and the gamma rates R_γ (bottom symbols scaled on the right axis) at Th = 0.6 (full circles), 0.75 (open circles), and 1.0 mV (squares), as a function of HV_{eff}, tested for the first η divions of the double-gap (left) and the four-gap (right) RPCs.

2016 JINST 11 C08008

The influence of the gamma background on ε_μ and $\langle C_s \rangle$ for the 100-GeV muons provided by the H4 beam line is shown in figures 9 and 10, respectively. For both detectors, we adjusted the threshold to 190 fC. We adjusted the intensity of the gamma rays emitted from the ^{137}Cs gamma source at the GIF++ (impinging on the RPCs) by three-step attenuations using tungsten filters of various thicknesses. We measured the maximum gamma rates present with the attenuation factors of 69 (blue squares) and 2.2 (red circles) as 110 and 1545 Hz cm^{-2} for the double-gap RPCs (placed relatively closer to the gamma source) and 72 and 1055 Hz cm^{-2} for the four-gap RPCs, respectively.

As shown in figures 9 and 10, we observed fairly insignificant shifts in $\mathrm{HV_{eff}}$ yielding $\varepsilon_\mu = 0.95$ (due to the presence of gamma rates of about 1 kHz cm^{-2}), while observing noticeable reductions in $\langle C_s \rangle$. The low sensitivity of the efficiency to the gamma rate should serve to guarantee a reliable operating condition for the trigger RPCs in the high-rate background environment in future CMS experiments.

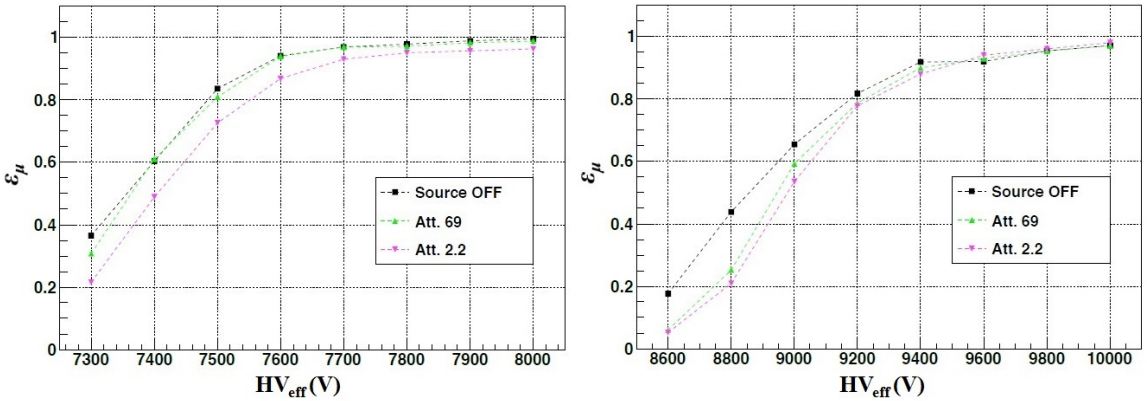

Figure 9. ε_μ for the 100-GeV muons provided by the H4 beam line as a function of $\mathrm{HV_{eff}}$, tested for the third η divisions of the double-gap (left) and the four-gap RPCs (right). The text describes the details for the symbols.

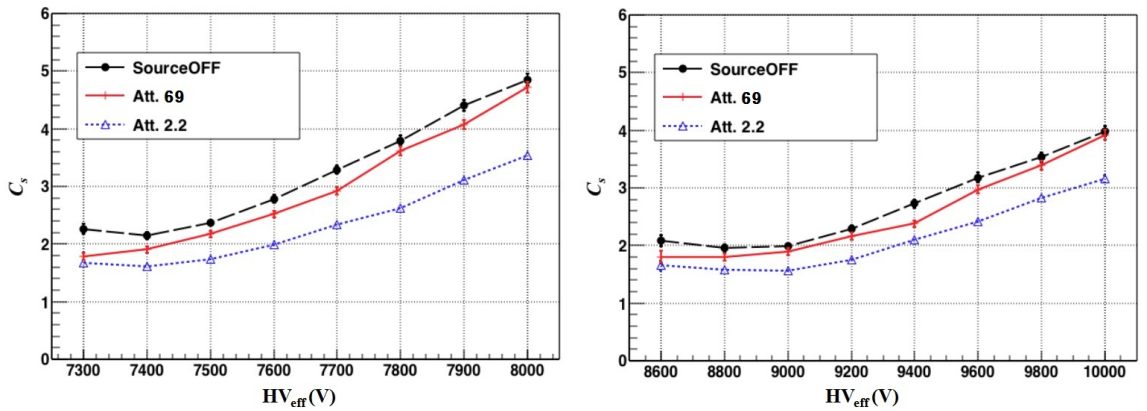

Figure 10. $\langle C_s \rangle$ for the 100-GeV muons provided by the H4 beam line as a function of $\mathrm{HV_{eff}}$, tested for the third η divisions of the double-gap (left) and the four-gap RPCs (right). The text describes the details for the symbols.

2016 JINST 11 C08008

4 Conclusions

In the present research, we examined two different phenolic RPC types with cosmic rays at Korea University and 100 GeV muons provided by the SPS H4 beam line at CERN. We examined the rate capabilities of the prototype RPCs with gamma-ray hits of maximum 1.5 kHz cm^{-2} provided by the ^{137}Cs gamma sources at Korea University and the GIF++ irradiation facility at CERN. We drew the following conclusions from the present research:

1. For the 1.6-mm double-gap RPC, a relatively high threshold value is preferred to suppress the magnitude of $\langle C_s \rangle$ and the rapid increase with $\mathrm{HV_{eff}}$. Fine adjustments of the threshold values in accordance with the strip pitches would be conducive to achieving a consistent hit structure over the whole detector surface.

2. The relatively large sensitivity of ε_μ to the threshold value for the four-gap RPC implied an advantage, namely enhancing the detector sensitivity by lowering the threshold. In the mid-section of the efficiency plateau, the gamma-induced currents drawn in the four-gap RPC were about one fourth of those drawn in the double-gap RPC. Considering the high particle rates expected at the position of the future RE3/1 and RE4/1 RPCs, the smaller avalanche charges of the four-gap RPCs appeared fairly advantageous to guarantee the longevity of the trigger RPCs.

3. For both RPC types, we observed quite insignificant shifts of the $\mathrm{HV_{eff}}$ curves due to the presence of the gamma rates of about 1 kHz cm^{-2}. The low sensitivity of the efficiencies to the gamma rate should guarantee a reliable operation of the trigger RPCs in the high-rate background environment in future CMS experiments.

Acknowledgments

This study was supported by the National Research Foundation of Korea (grant number NRF-2013R1A1A2060257). Most of all, we would like to give our special thanks to all team members dedicated the beam test and to the CERN EN and EP departments for the facility infrastructure support.

References

[1] P. Paolucci et al., *CMS Resistive Plate Chamber overview, from the present system to the upgrade phase I*, 2013 *JINST* **8** P04005 [PoS(RPC2012)004] [arXiv:1209.1941].

[2] CMS collaboration, *Performance Study of the CMS Barrel Resistive Plate Chambers with Cosmic Rays*, 2010 *JINST* **5** T03017 [arXiv:0911.4045].

[3] CMS collaboration, *CMS Physics : Technical Design Report Volume 1: Detector Performance and Software*, CERN-LHCC-2006-001, February 2006.

[4] CMS collaboration, *Provisional agenda for the thirty-second meeting of the Large Hadron Collider Committee to be held Thursday and Friday, 15 - 16 Jan 1998*, CERN-LHCC-97-32.

[5] CMS collaboration, *Observation of a new boson at a mass of 125 GeV with the CMS experiment at the LHC*, *Phys. Lett.* **B 716** (2012) 30 [arXiv:1207.7235].

2016 JINST 11 C08008

[6] M. Konecki, *The RPC based trigger for the CMS experiment at the LHC*, 2014 *JINST* **9** C07002.

[7] S. Costantini et al., *Uniformity and Stability of the CMS RPC Detector at the LHC*, 2012 *JINST* **8** P03017 [PoS(RPC2012)005] [arXiv:1209.1989].

[8] M. Tytgat et al., *The Upgrade of the CMS RPC System during the First LHC Long Shutdown*, 2013 *JINST* **8** T02002 [PoS(RPC2012)063] [arXiv:1209.1979].

[9] S.K. Park et al., *CMS endcap RPC gas gap production for upgrade*, 2012 *JINST* **7** P11013.

[10] *Technical Proposal for the Phase-II Upgrade of the CMS Detector*, CERN-LHCC-2015-010; LHCC-P-008.

[11] G.M. Pugliese on behalf of the CMS collaboration, *CMS RPC muon detector performance with 2010-2012 LHC data*, talk given at the *XII Workshop on Resistive Plate Chambers and Related Detector*, Beijing February 2014.

[12] S. Costantini on behalf of the CMS collaboration, *Radiation Background with the RPCs at the CMS Experiment*, talk given at the *XII Workshop on Resistive Plate Chambers and Related Detector*, Beijing February 2014.

[13] K.S. Lee, *Rate-capability study of a four-gap phenolic RPC with a* ^{137}Cs *source*, 2014 *JINST* **9** C08001.

[14] S.K. Park et al., *Test of a four-gap resistive plate chamber with cosmic muons and high-rate gamma rays*, *Nucl. Instrum. Meth.* **A 680** (2012) 134.

[15] R. Cardarelli, G. Aielli, P. Camarri, A. Di Ciaccio, L. Di Stante, B. Liberti et al., *Performance of RPCs and diamond detectors using a new very fast low noise preamplifier*, 2013 *JINST* **8** P01003.

2016 JINST 11 C08008